Efficiently Coupling Light to Superconducting Nanowire Single-Photon Detectors

Xiaolong Hu, *Student Member, IEEE*, Charles W. Holzwarth, Daniele Masciarelli, Eric A. Dauler, and Karl K. Berggren

***Abstract*—We designed superconducting nanowire single-photon detectors (SNSPDs) integrated with silver optical antennae for free-space coupling and a dielectric waveguide for fiber coupling. According to our finite-element simulation, (1) for the free-space coupling, the absorptance of the NbN nanowire for TM-polarized photons at the wavelength of 1550 nm can be as high as 96% by adding silver optical antennae; (2) for the fiber coupling, the absorptance of the NbN nanowire for TE-like-polarized photons can reach 76% including coupling efficiency at the wavelength of 1550 nm by adding a silicon nitride waveguide and an inverse-taper coupler.**

***Index Terms*—Niobium nitride, optical waveguides, plasmons, single-photon detectors.**

I. Introduction

INFRARED photon counting is more challenging compared with its visible counterpart because the energy of each quantum is smaller; however, in some applications such as fiber-based quantum-key distribution (QKD) systems [1] and photon-counting optical fiber communications [2], efficient infrared photon-counters are essential because the minimum absorption window for telecom fiber is at the wavelength of 1550 nm. Niobium nitride (NbN) superconducting nanowire single-photon detectors (SNSPDs) [3] are an emerging, ultrasensitive photon counting technology at infrared wavelengths. With its good detection efficiency, low dark-count rate, and high speed, an SNSPD has already been used in a recent demonstration of QKD [1]. In the past, our group demonstrated an SNSPD with 57% device efficiency at the wavelength of 1550 nm [4]; however, improving this device efficiency is important because some applications, such as linear optical quantum computing [5], require efficiency approaching 100%. Furthermore, efficiently coupling of light from free space or an optical fiber to an SNSPD is as important as improving its device efficiency. Device designs intended to improve the coupling efficiency, other than increasing the active area of the SNSPD, have not been previously reported.

The system detection efficiency or the total efficiency, η, of an SNSPD can be expressed as the product of three factors: $\eta = \eta_{\rm c} \times A \times P_{\rm r}$, where $\eta_{\rm c}$ is the coupling efficiency, the probability that an incident photon from free space or a fiber reaches the active area of the SNSPD; A is the absorptance of NbN, the probability that the photon is absorbed by NbN once it has reached the active area; $P_{\rm r}$ is the voltage-pulse generation probability for absorbing the photon. $A \times P_{\rm r}$ is referred to as the device efficiency. The expression for η not only illustrates the physical process of single-photon detection, but also suggests that from the perspective of system detection efficiency, $\eta_{\rm c}$, A, and $P_{\rm r}$ are equally important. This paper is devoted to designing SNSPDs with enhanced $\eta_{\rm c} \times A$ without increasing the nanowire width or length.

Enhancing $\eta_{\rm c} \times A$ of an SNSPD is not a trivial task because of two facts: firstly, the active area of SNSPDs is small—in practice, it is difficult to fabricate a long NbN meander to cover a large area without losing device efficiency. Up to now, the detector with the highest device efficiency is 3 μm by 3.3 μm [4], which is too small to achieve efficient coupling from free space or from a fiber because the spot size that one can obtain without adding additional losses is roughly on the same scale of the active area of this detector, limited by diffraction. Furthermore, the longer the NbN nanowire, the slower the detector: the speed of the detector is limited by its kinetic-inductance, which is proportional to the length of the nanowire [6]. Secondly, the NbN film used in an SNSPD is only a few nanometers thick; therefore, the incident photon can pass through the film with a significant probability. Intuitively speaking, to enhance $\eta_{\rm c} \times A$, one has to optimize the spatial overlap between the light and NbN nanowire, and make their interaction length as long as possible.

In this paper, we designed two novel device structures to enhance $\eta_{\rm c} \times A$ of SNSPDs, one for free-space coupling and another for fiber-coupling. For coupling light from free space, we designed an SNSPD integrated with silver optical antennae between adjacent nanowires. We will show that transverse-magnetic (TM)-polarized light can be efficiently focused onto the NbN nanowire, and the absorptance A at 1550 nm can be over 90%. Also, by increasing the width of the silver antennae and sacrificing a little absorptance A, the effective area of a detector can be expanded to enhance the coupling without increasing the length of the NbN nanowire. As the optical con-

Manuscript received August 22, 2008. First published June 30, 2009; current version published July 10, 2009. This work was supported in part by IARPA.

X. Hu and K. K. Berggren are with the Department of Electrical Engineering and Computer Science, Massachusetts Institute of Technology, Cambridge, MA 02139 USA (e-mail: XLHU@mit.edu).

C. W. Holzwarth is with the Department of Material Science and Engineering, Massachusetts Institute of Technology, Cambridge, MA 02139 USA.

D. Masciarelli was with the Department of Electrical Engineering and Computer Science, Massachusetts Institute of Technology, Cambridge, MA 02139, and with the Dipartimento di Elettronica, III Facoltà di Ingegneria, Politecnico di Torino, 24 Corso Duca degli Abruzzi, 10129 Torino, Italy.

E. A. Dauler is with the Department of Electrical Engineering and Computer Science, Massachusetts Institute of Technology, Cambridge, MA 02139, USA. He is also with the Lincoln Laboratory, Massachusetts Institute of Technology, Lexington, MA 02420 USA.

Color versions of one or more of the figures in this paper are available online at http://ieeexplore.ieee.org

Digital Object Identifier 10.1109/TASC.2009.2018035

stants of gold are very close to the optical constants of silver at 1550 nm [7], our discussion is also applicable for gold optical antennae integration, although the absorption of gold will be slightly stronger than silver at this wavelength. For coupling light from a single-mode optical fiber, we designed an SNSPD where the nanowire is integrated with a Si_3N_4 waveguide and an inverse-taper coupler. The light can be adiabatically coupled to the Si_3N_4 waveguide via the coupler, and eventually coupled to the NbN nanowire. We will show that the $\eta_c \times A$ of this waveguide-integrated SNSPD can be 76% for a transverse-electric (TE)-like optical mode.

II. Antenna-Integrated SNSPDs

In this section, we describe our design of antenna-integrated SNSPDs and evaluate its efficiency. We will show that the silver antennae can enhance the absorptance of NbN and enlarge the effective area of the detector, which may be useful for applications where free-space coupling is desired.

A. The Device and Illumination Structure

The device structure of an antenna-integrated SNSPD is schematically shown in Fig. 1(a). Compared with the detector integrated with a microcavity and an anti-reflection coating (ARC) that our group demonstrated in the past [4], the key element added here is a silver sub-wavelength grating between adjacent NbN nanowires. We call such a grating optical antennae because it can effectively collect TM-polarized incident photons as we will show below. For fabrication considerations, the silver grating layer is designed to connect with the silver reflector. We use 100-nm wide NbN nanowires with 200-nm pitch on sapphire substrate for illustrative purposes. On top of the NbN there is a 2-nm-thick layer of $NbNO_x$ (not shown). The cavity length l_c is defined as the distance between the top surface of $NbNO_x$ and the bottom surface of the reflector. Inside the cavity is hydrogen silsesquioxane (HSQ), commonly used as a spin-on, low-k dielectric and resist for electron-beam lithography. The gap between the silver grating and the adjacent NbN is noted as g.

The illumination scheme is also shown in Fig. 1(a). The detector is illuminated from the bottom through the ARC, and the wavelength used throughout this paper is 1550 nm. We consider two independent polarizations: TE polarization, in which the electrical field has only a z-component and TM polarization, in which the magnetic field has only a z-component.

B. Method of Simulation

We performed finite-element optical simulation using commercial software, Comsol Multiphysics [8]. We were able to simplify this simulation by simulating only one period of the whole structure and then applying periodic boundary conditions to the right and left boundaries. This simulation is equivalent to an infinitely extended periodic structure in the x-direction, and therefore it neglects any edge effects of the real meander [10].

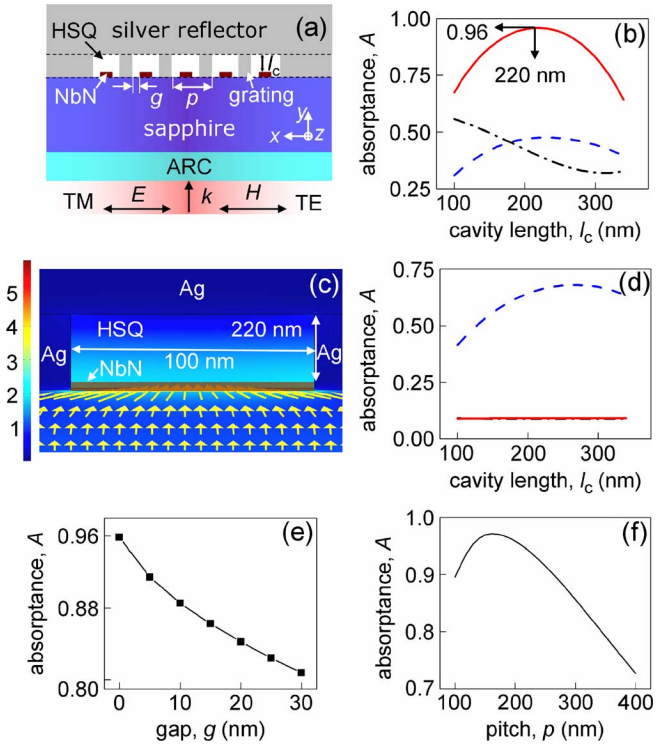

Fig. 1. (Color online) An optical antenna-integrated superconducting single-photon detector and its performance: (a) device cross section (not to scale); (b) absorptance for TM-polarization as a function of cavity length, l_c (solid line, $p = 200$ nm, $g = 0$), also compared with the detectors only integrated with a cavity (dashed line, $p = 200$ nm) or a grating (dash-dotted line, $p = 200$ nm, $g = 0$); (c) the electrical field magnitude distribution (surface, with arbitrary units) and optical power flow (arrows) near the NbN nanowire, and note that the figure is not to scale; (d) similar to (b), but for TE-polarization, and note that the solid line and the dash-dotted line are almost identical; (e) absorptance for TM-polarization as a function of the gap, g, and the line is for eye-guiding; (f) absorptance for TM-polarization as a function of the pitch, p, by varying the width of the silver antenna. We note here that although the simulation was done for p ranging from 100 nm to 400 nm, devices with smaller p are more difficult to fabricate.

TABLE I
Optical Refractive Indices

Material	Refractive index at 1550 nm
NbN [10]	5.23+ *i*5.82
$NbNO_x$ [10]	2.28
Sapphire [10]	1.75
HSQ [10]	1.39
Silver [7, 9]	0.51+ *i*10.72
Si_3N_4 [14]	1.98
SiON [14]	1.75

All of the optical constants used in this paper are listed in Table I.

C. Results and Discussions

The enhancement of the absorptance by antenna-integration is large, which can be seen in Fig. 1(b). The absorptance of NbN

as a function of the cavity length for TM-polarization is shown as the solid line. In this idealized model with $p = 200$ nm pitch and $g = 0$, the absorptance peaks at $l_c = 220$ nm and the corresponding absorptance is 0.96. Perfect absorptance is not achieved due to a small residual reflection by the silver grating and the absorption of the silver. As a comparison, the absorptance of NbN with the cavity only and with the silver grating only was also obtained by simulation, shown as the dashed line and the dash-dotted line in Fig. 1(b), respectively. With neither a reflector nor a grating, the absorptance is 0.19, obtained by simulation.

The ability of the grating to collect the TM-polarized photons onto the NbN can be clearly seen by looking at optical power flow shown as arrows in Fig. 1(c): the photons are concentrated in the slot between the silver where the NbN is located. As a comparison, similar simulations were also performed for TE-polarization. As shown in Fig. 1(d), the absorptance of NbN is greatly reduced by adding the grating because the grating essentially blocks the TE-polarized incident photons. The physics of the absorptance-enhancement of TM-polarization and suppression of TE-polarization can be understood by viewing the silver grating as an array of metal-insulator-metal surface-plasmon waveguides [11]. Such waveguides support modes with TM-polarization but not TE-polarization.

We also studied the effect of the gap between the silver and the NbN nanowire on absorptance. The reason for this study is that although there may be a thin $NbNO_x$ layer covering the NbN, we do not know whether this layer is sufficient to electrically insulate the NbN from the silver. In an experiment, we may need a spacer between the silver and the adjacent NbN nanowire. Therefore one concern is whether this gap between silver and NbN, g, will significantly reduce the absorptance of NbN. As shown in Fig. 1(e), the absorptance A of NbN is plotted as a function of the gap g. The absorptance does reduce with increasing the gap because the field of the plasmon mode is strongest at the edge of the silver, and therefore, the gap reduces the spatial overlap between NbN nanowire and the optical mode. However, even with a 30-nm gap, the absorptance is still over 0.8, which is larger than the optimized absorptance obtained with only an integrated microcavity.

The antenna-integrated SNSPD offers the possibility of enlarging the equivalent active area of the detector without increasing the length of the NbN nanowire or losing too much absorptance. We expanded the silver grating in the x-direction, and studied the absorptance vs. the pitch, p, while keeping other parameters unchanged. Shown in Fig. 1(f), as the pitch increases to 400 nm by increasing the width of the silver antenna to 300 nm, the absorptance is gradually reduced to 0.73. With sacrificing some absorptance, the total area of the detector is doubled, which makes coupling easier, and therefore, increases the coupling efficiency, η_c. As a result, $\eta_c \times A$ may be improved for instances where a larger spot-size is desirable.

III. Waveguide-Integrated SNSPDs

In this section, we describe our design of a waveguide-integrated SNSPDs and evaluate its efficiency. We will show that the inverse-taper coupler and the waveguide can increase the coupling efficiency with a single-mode fiber and enhance the absorptance of NbN, which is preferable for applications such as fiber-based QKD where fiber-based coupling is desired.

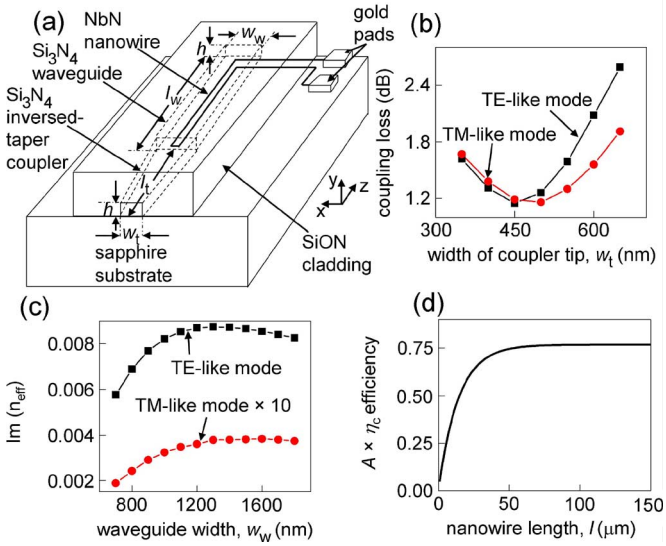

Fig. 2. (Color online) A waveguide-integrated superconducting single-photon detector and its performance: (a) device structure; (b) the coupling loss of the inverse-taper coupler for TE- and TM-like polarizations; (c) the imaginary part of the effective refractive index of the waveguide with niobium nitride (NbN) nanowires for TE- and TM-like polarizations; (d) $\eta_c \times A$ efficiency as a function of the length of the NbN nanowire l.

A. The Device Structure

A waveguide-integrated SNSPD that we designed is shown schematically in Fig. 2(a). The NbN nanowire is no longer a meander structure as in a traditional SNSPD; instead, it is a straight nanowire wound only once. On top of the NbN nanowire, a Si_3N_4 waveguide is integrated with a SiON cladding layer. Furthermore, the beginning of the waveguide is tapered in order to facilitate the coupling of light from a single-mode fiber [12]. Different from the traditional SNSPD, in which the light is coupled from the top or bottom, here the light is coupled from the facet of the inverse-taper coupler, then adiabatically coupled to the Si_3N_4 waveguide, and eventually coupled to the NbN nanowire.

We designed the taper to minimize the coupling loss and the waveguide to maximize the absorption per unit length of the NbN nanowire in order to reduce its total length. For illustrative purpose, we use 100-nm-wide NbN nanowires spaced with a 100-nm gap. The thickness of the Si_3N_4 layer for both the waveguide and the coupler is 300 nm. We found by simulation that the optimized $\eta_c \times A$ does not differ significantly for different thicknesses around 300 nm. The width of the coupler tip w_t can be designed to increase or reduce its mode size to match the mode from the fiber. The width of the waveguide is noted as w_w, which can be designed to maximize the absorption of NbN by controlling the size of the supported mode of the waveguide. The length of the taper l_t, dependent on w_t and w_w, must be long enough to ensure that the coupling from the inversed taper

to the waveguide is adiabatic. The length of the waveguide $l_{\rm w}$ is approximately half of the length of the nanowire, l, i.e., $l \approx 2l_{\rm w}$.

B. Method of Simulation and Calculation

We first consider the coupling of the light from the single-mode fiber with a 9.8 μm mode-field diameter (MFD) to the inverse-taper coupler. The coupling efficiency η_c can be calculated by [13] $\eta_{\rm c} = |a|^2 N/P$, where $N = \{\int_{S\to\infty}(\vec{E}^*_{\rm T,t} \times \vec{H}_{\rm T,t}) \cdot \hat{z} dS\}/2$, $P = \{\int_{S\to\infty}(\vec{E}^*_{\rm T,f} \times \vec{H}_{\rm T,f}) \cdot \hat{z} dS\}/2$, $a = \{\int_{S\to\infty}(\vec{E}_{\rm T,f} \times \vec{H}^*_{\rm T,t}) \cdot \hat{z} dS\}/(2N)$, $\vec{E}_{\rm T,t(f)}$ and $\vec{H}_{\rm T,t(f)}$ are the transverse electrical and magnetic fields of the coupler tip (fiber), respectively, dS is the differential cross-sectional-area element. Here, we use a Gaussian profile and linear polarization mode to approximate the mode of the fiber and obtain the mode of the coupler tip via finite-element method using Comsol Multiphysics. In our simulation, we chose S as a 20 μm by 20 μm square to ensure the field outside this area is negligibly weak. The refractive indices used can be found in Table I. In practice, the refractive indices for $\rm Si_3N_4$ and SiON can be controlled by controlling the flow ratio and the pressure of the gases in the PECVD process. The backreflection due to the index mismatch between the fiber and the inverse-taper coupler is estimated to be $\sim$10%, and can be experimentally eliminated by adding a quarter-wavelength ARC on the taper facet. Therefore, the coupling efficiency calculated above has not taken this backreflection into account.

We then design the waveguide with NbN nanowire by varying $w_{\rm w}$. For each $w_{\rm w}$, we use finite-element analysis to find the complex effective index $n_{\rm eff}$ of the waveguide, composed of the $\rm Si_3N_4$ core, the SiON cladding and NbN. The larger the imaginary part $\rm Im(n_{eff})$, the stronger the absorption in the NbN. In this way, we can find the optimized $w_{\rm w}$, which can yield the largest $\rm Im(n_{eff})$. The absorptance of the NbN is calculated by $A = 1 - \exp[-(2\pi/\lambda_0) \times \rm Im(n_{eff}) \times 2 \times \it l]$, where λ_0 is the wavelength (1.55 μm), and l is the length of the nanowire.

C. Results and Discussions

The coupling loss as a function of the coupler-tip width $w_{\rm t}$ is plotted in Fig. 2(b). As the width of the coupler tip increases, the mode size decreases. When the mode size of the coupler at its tip becomes similar to the mode size of the single-mode fiber, the coupling loss is minimized. One can see that this minimized loss for both TE- and TM-like polarizations is about 1.2 dB when the $w_{\rm t}$ is 450 nm for TE-like and 500 nm for TM-like, respectively. In this region, the coupling loss is quite insensitive to variations in width. This residual coupling loss is due to the difference of the shape between the modes of the fiber and of the coupler although the mode sizes are similar.

The imaginary part of the effective index of the waveguide $\rm Im(n_{eff})$ is plotted in Fig. 2(c) as a function of the width of the waveguide $w_{\rm w}$. As $w_{\rm w}$ increases, more light is confined within the $\rm Si_3N_4$ layer, and therefore the spatial overlap between NbN and the mode increases; however, further increase of $w_{\rm w}$ results in a drop of $\rm Im(n_{eff})$ because the mode is spread along the $\rm Si_3N_4$ core, its overlap with NbN at the center becomes smaller. Thus, $\rm Im(n_{eff})$ reaches its maximum 0.00875 when $w_{\rm w}$ is 1300 nm for TE-like polarization. The absorption for the TE-like mode is much stronger than TM-like mode because the electrical field of TM-like field is in the y-direction, and in this direction, NbN is only 4 nm thick. To adiabatically couple the light from the 450- or 500-nm wide coupler tip to the 1300-nm wide waveguide, we use a 500-μm long inverse taper.

In Fig. 2(d), we then plot optimized $\eta_{\rm c} \times A$ for TE-like mode as a function of l. The $\eta_{\rm c} \times A$ exponentially increases with l, then at $l \sim 50$ μm, it starts to saturate, slowly approaching its upper bound 0.76: further increasing the nanowire length does not significantly increase the $\eta_{\rm c} \times A$. We note here that we have not taken into account the material optical loss of $\rm Si_3N_4$ because it can be made as small as 5 dB/cm by the PECVD process followed by annealing [14]. The total length of the coupler and the waveguide is about 525 μm, and the estimated additional material loss is only $\sim$0.2 dB.

Let us compare the performance of the waveguide-integrated SNSPD and the traditional cavity-integrated SNSPD [4], for TE- or TM-like polarizations. As mentioned above, the waveguide-integrated SNSPD can achieve a $\eta_{\rm c} \times A$ of 0.76 with a 50-μm long NbN nanowire, and is directly coupled with a single-mode fiber. For cavity-integrated SNSPDs, on the other hand, the optimized absorptance is 0.68, independent of the total length of the nanowire. In contrast, the coupling efficiency is dependent on the length of the nanowire: (1) a 3 μm-by-3 μm SNSPD coupled with a single spatial mode with $\rm MFD = 9.8$ μm, a similar mode-size with a single-mode fiber, the optimized coupling efficiency is $\sim$0.15, and therefore, $\eta_{\rm c} \times A$ is $\sim$0.10; (2) a 10 μm-by-10 μm SNSPD coupled with the same spatial mode, the optimized coupling efficiency is $\sim$0.85, and therefore, $\eta_{\rm c} \times A$ is $\sim$0.58; (3) a 3 μm-by-3 μm SNSPD coupled with a single spatial mode with $\rm MFD = 5$ μm, a similar mode-size with a fiber-focuser at its beam waist, the optimized coupling efficiency is $\sim$0.5, and therefore, $\eta_{\rm c} \times A$ is $\sim$0.34; (4) a 10 μm-by-10 μm SNSPD coupled with the same spatial mode, the coupling efficiency is $\sim$1, and therefore, $\eta_{\rm c} \times A$ is $\sim$0.68. Thus one can see that $\eta_{\rm c} \times A$ of the waveguide-integrated SNSPD exceeds the $\eta_{\rm c} \times A$ in the four cases without waveguide coupling. Although the total length of the NbN nanowire in a 3 μm-by-3 μm SNSPD is about 45 μm, similar to the length of the nanowire in a waveguide-integrated SNSPD, its $\eta_{\rm c} \times A$ is much smaller, even coupled with a fiber focuser. Thus, we conclude that the waveguide-integrated SNSPD can work with simultaneously high speed and high $\eta_{\rm c} \times A$, and it is directly coupled with a single-mode fiber.

The fabrication process of the waveguide-integrated SNSPDs is slightly more complicated than the process of the traditional cavity-integrated SNSPDs [4]. To fabricate the waveguide-integrated SNSPD, we need to perform e-beam lithography twice: first to define the NbN nanowire, and second to define the $\rm Si_3N_4$ waveguide, which must be aligned with the nanowire.

The waveguide-integrated SNSPDs are ideal for a system that is already fiber-coupled, for instance, a fiber-based QKD system. Free-space systems can benefit from the convenience of fiber-delivery to the detector without using beam-steering optics or a telescope-mounted cryostat. More importantly, the waveguide-integrated SNSPDs are compatible with various

photonics-on-a-chip technologies. For instance, one can conveniently integrate it with one or multiple ring resonators so that the SNSPDs acquire the ability to distinguish the wavelength of the incident photons. This feature could facilitate SNSPDs for applications in integrated wavelength division multiplexing systems.

IV. Final Remarks and Conclusion

As a final remark, from the point view of system detection efficiency, these two novel designs can outperform the traditional cavity-integrated SNSPD only if P_{r} is not significantly reduced. Up to now, the SNSPD community does not have too much insight on what factors determine P_{r}, and even why P_{r} is not equal to 1. Therefore, it requires more study. In the past, our observation showed that P_{r} may depend on the electrical field distribution along x-direction within the NbN nanowire [15]. We checked this electrical field distribution in our simulation: for an antenna-integrated SNSPD, the electrical-field distribution along x-direction for TM-polarization is similar to that for TE-polarization in a traditional cavity-integrated SNSPD; for a waveguide-integrated SNSPD, the electrical-field distribution along x-direction for TE-like mode is similar to that for TM-polarization in a traditional cavity-integrated SNSPD. Therefore, we suspect that P_{r} will not be significantly affected. However, in order to give a conclusive answer, we must fabricate the devices and test them.

In summary, we have proposed two novel designs of SNSPDs: one is antenna-integrated SNSPDs for free-space coupling with absorptance A of 0.96; another is waveguide-integrated SNSPDs for fiber coupling with $\eta_{\mathrm{c}} \times A$ of 0.76. We compared them with the traditional cavity-integrated SNSPDs, and showed that both antenna- and waveguide-integrated SNSPDs can achieve more efficient coupling and larger absorptance without increasing the length of the NbN nanowire. Therefore, they can work simultaneously with high efficiency and fast speed. We believe that with these improved performances, the antenna- and waveguide-integrated SNSPDs may enable applications such as long-distance QKD, ultrafast time-resolved photoluminescence measurement, and characterization of entangled-photon sources at infrared wavelengths.

References

[1] H. Takesue, S. W. Nam, Q. Zhang, R. H. Hadfield, T. Honjo, K. Tamaki, and Y. Yamamoto, "Quantum key distribution over a 40-dB channel loss using superconducting single-photon detectors," *Nature Photonics*, vol. 1, pp. 343–348, 2007.

[2] B. S. Robinson, A. J. Kerman, E. A. Dauler, R. J. Barron, D. O. Caplan, M. L. Stevens, J. J. Carney, S. A. Hamilton, J. K. Yang, and K. K. Berggren, "781 Mbit/s photon-counting optical communications using a superconducting nanowire detector," *Opt. Lett.*, vol. 31, pp. 444–446, 2006.

[3] G. N. Gol'tsman, O. Okunev, G. Chulkova, A. Lipatov, A. Semenov, K. Smirnov, B. Voronov, A. Dzardanov, C. Williams, and R. Sobolewski, "Picosecond superconducting single-photon optical detector," *Appl. Phys. Lett.*, vol. 79, pp. 705–707, 2001.

[4] K. M. Rosfjord, J. K. W. Yang, E. A. Dauler, A. J. Kerman, V. Anant, B. M. Voronov, G. N. Gol'tsman, and K. K. Berggren, "Nanowire single-photon detector with an integrated optical cavity and anti-reflection coating," *Opt. Express*, vol. 14, p. 527, 2006.

[5] E. Knill, R. Laflamme, and G. J. Milburn, "A scheme for efficient quantum computation with linear optics," *Nature*, vol. 409, pp. 46–52, 2000.

[6] A. J. Kerman, E. A. Dauler, W. E. Keicher, J. K. W. Yang, K. K. Berggren, G. N. Gol'tsman, and B. M. Voronov, "Kinetic-inductance-limited reset time of superconducting nanowire photon counters," *Appl. Phys. Lett.*, vol. 88, p. 111116, 2006.

[7] D. W. Lynch and W. R. Hunter, "Comments on the optical constants of metals and an introduction to the data for several metals," in *Handbook of Optical Constants of Solids*, E. D. Palik, Ed. New York: Academic Press, Inc., 1998, pp. 257–367.

[8] [Online]. Available: http://www.comsol.com/

[9] The optical constants for silver at 1550 nm given in reference [7] are two sets of data: $n = 0.469, k = 9.32$; $n = 0.514, k = 10.8$. The numbers we used are given in the table.

[10] A. Vikas, "Engineering the Optical Properties of Subwavelength Devices and Materials," Ph.D. thesis, Massachusetts Institute of Technology, , 2007.

[11] J. A. Dionne, L. A. Sweatlock, H. A. Atwater, and A. Polman, "Plasmon slot waveguides: Towards chip-scale propagation with subwavelength-scale localization," *Phys. Rev. B*, vol. 73, p. 035407, 2006.

[12] V. R. Almeida, R. R. Panepucci, and M. Lipson, "Nanotaper for compact mode conversion," *Opt. Lett.*, vol. 28, p. 1302, 2003.

[13] See, for exampleA. W. Snyder and J. D. Love, Optical Waveguide Theory pp. 420–441.

[14] A. Zhang, K. T. Chan, M. S. Demokan, V. W. C. Chan, P. C. H. Chan, and A. H. P. Chan, "Annealing effects on the loss and birefringence of silicon oxynitride rectangular optical waveguide," *Appl. Phys. Lett.*, vol. 87, p. 101105, 2005.

[15] V. Anant, A. J. Kerman, E. A. Dauler, J. K. W. Yang, K. M. Rosfjord, and K. K. Berggren, "Optical properties of superconducting nanowire single-photon detectors," *Opt. Express*, vol. 16, pp. 10750–10761, 2008.